IL NUOVO CIMENTO Vol. 32 C, N. 5-6 Settembre-Dicembre 2009
DOI 10.1393/ncc/i2010-10524-2

Colloquia: LaThuile09

# Hadronic physics with KLOE

F. Ambrosino(3)(4), A. Antonelli(1), M. Antonelli(1), F. Archilli(8)(9), P. Beltrame(2), G. Bencivenni(1), S. Bertolucci(1), C. Bini(6)(7), C. Bloise(1), S. Bocchetta(10)(11), F. Bossi(1), P. Branchini(11), G. Capon(1), T. Capussela(1), F. Ceradini(10)(11), P. Ciambrone(1), E. De Lucia(1), A. De Santis(6)(7), P. De Simone(1), G. De Zorzi(6)(7), A. Denig(2), A. Di Domenico(6)(7), C. Di Donato(4), B. Di Micco(10)(11), M. Dreucci(1), G. Felici(1), S. Fiore(6)(7), P. Franzini(6)(7), C. Gatti(1), P. Gauzzi(6)(7), S. Giovannella(1)(*), E. Graziani(11), G. Lanfranchi(1), J. Lee-Franzini(1)(12), M. Martini(1)(5), P. Massarotti(3)(4), S. Meola(3)(4), S. Miscetti(1), M. Moulson(1), S. Müller(2), F. Murtas(1), M. Napolitano(3)(4), F. Nguyen(10)(11), M. Palutan(1), E. Pasqualucci(7), A. Passeri(11), V. Patera(1)(5), P. Santangelo(1), B. Sciascia(1), T. Spadaro(1), M. Testa(6)(7), L. Tortora(11), P. Valente(7), G. Venanzoni(1), R. Versaci(1)(5) and G. Xu(1)(13)

(1) *Laboratori Nazionali di Frascati dell'INFN - Frascati, Italy*

(2) *Institut für Kernphysik, Johannes Gutenberg Universität - Mainz, Germany*

(3) *Dipartimento di Scienze Fisiche dell'Università "Federico II" - Napoli, Italy*

(4) *INFN, Sezione di Napoli - Napoli, Italy*

(5) *Dipartimento di Energetica dell'Università "La Sapienza" - Rome, Italy*

(6) *Dipartimento di Fisica dell'Università "La Sapienza" - Rome, Italy*

(7) *INFN, Sezione di Roma - Rome, Italy*

(8) *Dipartimento di Fisica dell'Università "Tor Vergata" - Rome, Italy*

(9) *INFN, Sezione di Roma Tor Vergata - Rome, Italy*

(10) *Dipartimento di Fisica dell'Università "Roma Tre" - Rome, Italy*

(11) *INFN, Sezione di Roma Tre - Rome, Italy*

(12) *Physics Department, State University of New York at Stony Brook Stony Brook, NY, USA*

(13) *Institute of High Energy Physics of Academica Sinica - Beijing, China*

(ricevuto il 10 Novembre 2009; pubblicato online il 15 Gennaio 2010)

(*) E-mail: simona.giovannella@lnf.infn.it

 

**Summary.** — The KLOE experiment has collected 2.5 $\text{fb}^{-1}$ of $e^+e^-$ collisions at the $\phi$ peak and about 300 $\text{pb}^{-1}$ in the center-of-mass energy region 1000–1030 MeV. Data taken on peak are used to study the properties of light scalar and pseudoscalar mesons, produced through $\phi$ radiative decays, and to precisely measure the pion form factor using Initial State Radiation events. Energy scan data are used to measure the cross-section of the process $e^+e^- \to \omega\pi^0$ as a function of the center-of-mass energy and to perform a preliminary study of the reaction $e^+e^- \to e^+e^-\pi^0\pi^0$.

PACS 13.66.Bc – Hadron production in $e^+e^-$ interactions.

## 1. – Introduction

The high statistics collected by the KLOE experiment provides precise measurements of fundamental properties and dynamics of light mesons, thus offering an important testing ground for non-perturbative QCD and Standard Model tests. At the same time, studies on the meson internal structure gives important information to the long-lasting debates on the existence of exotic particles.

## 2. – Light scalar mesons

The still unresolved structure of these states is studied either through electric dipole transitions such as $\phi \to a_0(980)\gamma$, looking at the mass spectrum of the scalar meson decay products, or with the search for processes like $\phi \to [a_0(980) + f_0(980)]\gamma \to K\bar{K}\gamma$ and $\gamma\gamma \to \sigma(600) \to \pi\pi$.

**2**˙1. $\phi \to a_0(980)\gamma \to \eta\pi^0\gamma$. – Two independent analyses using $\eta \to \gamma\gamma$ or $\eta \to \pi^+\pi^-\pi^0$ decays are performed from a sample of 410 $\text{pb}^{-1}$ [1]. Both analyses share the requirement of five photons from the interaction point. Two tracks of opposite charge pointing to the interaction region are also required for the second channel. At the end of the analysis, after applying kinematical cuts to reduce background contamination, the fully neutral channel has a larger number of signal events $(13,269 \pm 192)$ and higher background contamination ($\sim 50\%$) while for the $\eta \to \pi^+\pi^-\pi^0$ both quantities are reduced by a factor 3.6. The absence of a major source of interfering background allows to obtain the branching fraction directly from event counting for both channels:

$$BR(\phi \to \eta\pi^0\gamma) = 7.01 \pm 10_{\text{stat}} \pm 20_{\text{syst}} \qquad (\eta \to \gamma\gamma), \tag{1}$$

$$BR(\phi \to \eta\pi^0\gamma) = 7.12 \pm 13_{\text{stat}} \pm 22_{\text{syst}} \qquad (\eta \to \pi^+\pi^-\pi^0). \tag{2}$$

The two samples lead to consistent branching ratio values, thus a combined fit of the two spectra is performed. The couplings, fitted according to the Kaon Loop [2] and the No Structure [3] models, point to a sizeable $s\bar{s}$ content of the $a_0(980)$.

**2**˙2. *Search for* $\phi \to K\bar{K}\gamma$. – In this process, never been observed, the $K\bar{K}$ system has scalar quantum numbers, therefore it is expected to proceed through the $\phi \to [a_0(980) + f_0(980)]\gamma \to K\bar{K}\gamma$ decay chain.

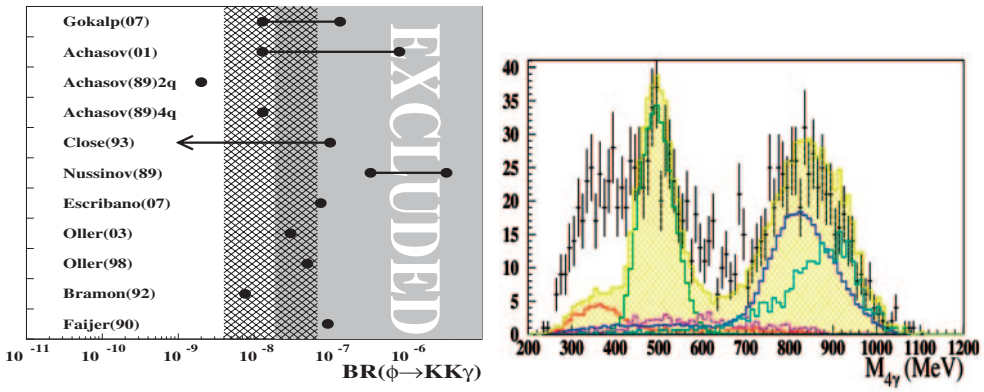


Fig. 1. – Left: excluded region at 90% CL for $BR(\phi \to K\bar{K}\gamma)$, compared with theoretical estimates and with KLOE predictions from $\phi \to f_0(980)\gamma \to \pi\pi\gamma$ and $\phi \to a_0(980)\gamma \to \eta\pi\gamma$ (hatched). Right: fit to $M_{4\gamma}$ with $\phi$ decays and $e^+e^-$ annihilation processes for data taken at 1 GeV.

The selected channel for this search is $\phi \to K_S K_S \gamma \to \pi^+\pi^-\pi^+\pi^-\gamma$. The main backgrounds are the resonant $e^+e^- \to \phi\gamma \to K_S K_L \gamma$ and the continuum $e^+e^- \to \pi^+\pi^-\pi^+\pi^-\gamma$ processes. Monte Carlo (MC) signal has been simulated according to phase space and radiative decay dynamics. Selection cuts have been optimized on MC.

From an integrated luminosity of $2.2\,\mathrm{fb}^{-1}$, 5 candidate events are found in data, while $3.2 \pm 0.7$ events are expected from MC [4]. This leads to $BR(\phi \to K\bar{K}\gamma) < 1.9 \times 10^{-8}$ at the 90% CL. Figure 1, left, compares this measurement with the predictions of various theoretical models. Some of them are excluded. The present upper limit is consistent with the $BR(\phi \to K\bar{K}\gamma)$ prediction computed with $f_0(980)$ and $a_0(980)$ couplings measured by KLOE [5, 6, 1].

**2˙3.** *Search for* $\gamma\gamma \to \sigma(600) \to \pi^0\pi^0$. – While there is a long debate on the observation of the $\sigma(600)$ as a bound $\pi^+\pi^-$ state, there is no direct evidence for the $\sigma(600) \to \pi^0\pi^0$ decay. At DAΦNE, the detection of the process $e^+e^- \to e^+e^-\pi^0\pi^0$ implies the intermediate process $\gamma\gamma$ to a scalar meson state. From a sample of $11\,\mathrm{pb}^{-1}$ of data taken at $\sqrt{s} = 1\,\mathrm{GeV}$, the feasibility study of the $\pi^0\pi^0 \to 4\gamma$'s invariant mass ($M_{4\gamma}$) spectrum, without tagging $e^+$ or $e^-$ in the final state, is performed. Preliminary results show an excess of events in the $M_{4\gamma}$ region below 400 MeV, where the contribution from the $\sigma(600)$ is expected, that is not explained by $\phi$ decays or $e^+e^-$ annihilation processes. This preliminary work is encouraging and motivates the analysis extension to the whole sample of $240\,\mathrm{pb}^{-1}$ collected by KLOE at $\sqrt{s} = 1\,\mathrm{GeV}$.

## 3. – The $\eta \to \pi^+\pi^-e^+e^-$ decay

The $\eta \to \pi^+\pi^-e^+e^-$ decay allows to probe the structure of the $\eta$ meson [7], to compare the predictions of the branching ratio value based on Vector Meson Dominance model and Chiral Perturbation Theory [8-11] and to study $CP$ violation beyond the prediction of the Standard Model by measuring the angular asymmetry between pions and electrons decay planes [12].

The analysis has been performed on $1733\,\mathrm{pb}^{-1}$ [13]. The events are required to have at least four tracks coming from a cylinder around the Interaction Point. A cluster not

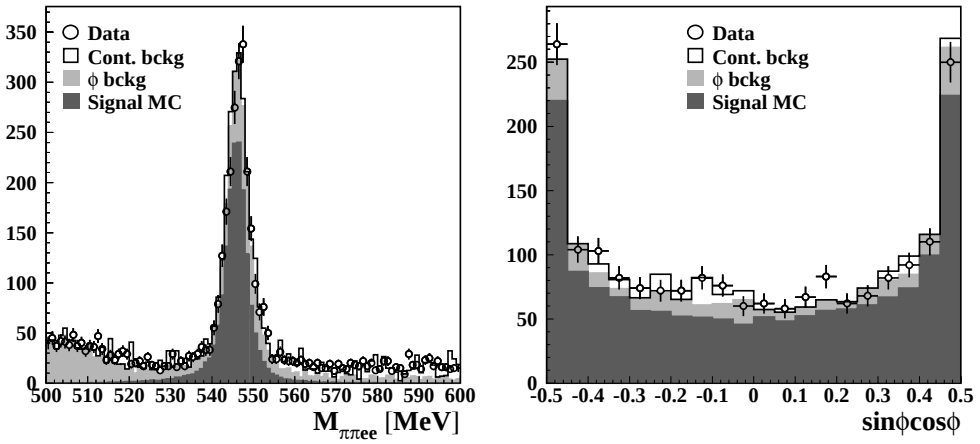


Fig. 2. – Left: fit to the invariant mass of the four selected tracks. Right: distribution of the $\sin\phi\cos\phi$ variable in the signal region. Dots: data. The black histogram is the expected distribution, *i.e.* signal MC (dark grey), $\phi$ background (light grey) and background in the continuum (white).

associated to any track, having time compatible with the photon time of flight, energy of at least 250 MeV and in the polar-angle range (23°–157°), is also required.

Background sources can be grouped into $\phi$-decays and events in the continuum. The former is mainly due to $\phi \to \pi^+\pi^-\pi^0$ events (with $\pi^0$ Dalitz decay) and to $\phi \to \eta\gamma$ events either with $\eta \to \pi^+\pi^-\pi^0$ (with $\pi^0$ Dalitz decay) or with $\eta \to \pi^+\pi^-\gamma$ (with photon conversion on the beam pipe). The latter comes mainly from $e^+e^- \to e^+e^-(\gamma)$ events. Because of poor MC statistics, they have been studied using off-peak data taken at $\sqrt{s} = 1\,\text{GeV}$, where $\phi$ decays are negligible. Backgrounds are reduced applying cuts on track momenta and reconstructing the invariant mass and the distance of the candidate electron pairs on the beam pipe to remove photon conversions.

Background contribution is evaluated performing a fit on the sidebands of the $\pi^+\pi^-e^+e^-$ invariant mass after the cuts on track momenta with background shapes. The output of the fit ($P(\chi^2) = 0.35$) is shown in the left panel of fig. 2. For the signal estimate we limit ourselves to the region $[535, 555]\,\text{MeV}$ and perform the event counting after background subtraction. The resulting value obtained for the branching ratio is

$$BR(\eta \to \pi^+\pi^-e^+e^-\gamma) = (26.8 \pm 0.9_{\text{stat}} \pm 0.7_{\text{syst}}) \times 10^{-5}. \tag{3}$$

The decay plane asymmetry is calculated starting from the momenta of the four particles and is expressed as a function of the angle $\phi$ between the pion and the electron planes in the $\eta$ rest frame. The value obtained is

$$\mathcal{A}_\phi = (-0.6 \pm 2.5_{\text{stat}} \pm 1.8_{\text{syst}}) \times 10^{-2}, \tag{4}$$

which is the first measurement of this asymmetry. The distribution of the $\sin\phi\cos\phi$ variable is shown in the right panel of fig. 2.

TABLE I. – *Fit results for the evaluation of the $\eta'$ gluonium content. In the first column, only the first two parameters are left free.*

| Parameter | KLOE published | KLOE update | KLOE update (no glue) |
|---|---|---|---|
| $Z^2_{\eta'}$ | $0.14 \pm 0.04$ | $0.12 \pm 0.04$ | 0 (fixed) |
| $\varphi_P$ | $(39.7 \pm 0.7)^\circ$ | $(40.4 \pm 0.6)^\circ$ | $(41.4 \pm 0.5)^\circ$ |
| $Z_{NS}$ | $0.91 \pm 0.05$ | $0.94 \pm 0.03$ | $0.93 \pm 0.02$ |
| $Z_S$ | $0.89 \pm 0.07$ | $0.83 \pm 0.05$ | $0.82 \pm 0.05$ |
| $\varphi_V$ | $3.2^\circ$ | $(3.32 \pm 0.09)^\circ$ | $(3.34 \pm 0.09)^\circ$ |
| $m_s/m$ | $1.24 \pm 0.07$ | $1.24 \pm 0.07$ | $1.24 \pm 0.07$ |
| $P(\chi^2)$ | 49% | 20.5% | 0.5% |

## 4. – Search for gluonium in $\eta'$

The $\eta'$-meson, being almost a pure $SU(3)$ singlet, is a good candidate for a sizeable gluonium content. In this hypothesis, the $\eta$ and $\eta'$ wave functions can be written in terms of the $u, d$ quark wave function ($|q\bar{q}\rangle = \frac{1}{\sqrt{2}}(|u\bar{u}\rangle + |d\bar{d}\rangle)$), the strange component ($|s\bar{s}\rangle$) and the gluonium ($|GG\rangle$) [14]:

$$|\eta'\rangle = \cos\varphi_G \sin\varphi_P \, |q\bar{q}\rangle + \cos\varphi_G \cos\varphi_P \, |s\bar{s}\rangle + \sin\varphi_G \, |GG\rangle, \tag{5}$$

$$|\eta\rangle = \cos\varphi_P \, |q\bar{q}\rangle - \sin\varphi_P \, |s\bar{s}\rangle, \tag{6}$$

where $\varphi_P$ is the $\eta$-$\eta'$ mixing angle and $Z^2_G = \sin^2\varphi_G$ is the gluonium fraction in the $\eta'$-meson.

From the study of $\phi \to \eta'\gamma \to \pi^+\pi^-7\gamma$'s and $\phi \to \eta\gamma \to 7\gamma$'s decays, the ratio $R_\phi = BR(\phi \to \eta'\gamma)/BR(\phi \to \eta\gamma)$ has been measured [15]: $R_\phi = (4.77 \pm 0.09_{\text{stat}} \pm 0.19_{\text{syst}}) \times 10^{-3}$. Using the approach of refs. [16,17], where the $SU(3)$ breaking is taken into account via the constituent quark mass ratio $m_s/\bar{m}$, $R_\phi$ can be parametrized as

$$R_\phi = \cot^2\varphi_P \cos^2\varphi_G \left(1 - \frac{m_s}{\bar{m}} \frac{C_{NS}}{C_S} \frac{\tan\varphi_V}{\sin 2\varphi_P}\right)^2 \left(\frac{p_{\eta'}}{p_\eta}\right)^3; \tag{7}$$

$p_{\eta'}$ and $p_\eta$ are the momenta of the $\eta'$- and $\eta$-meson, respectively, $\varphi_V$ is the $\phi$-$\omega$ mixing angle and $C_{NS}, C_S$ takes into account the vector and pseudoscalar wave function overlap. Combining our $R_\phi$ result with other experimental constraints and using the corresponding $SU(3)$ relations between decay modes [17, 18], we found a $3\,\sigma$ evidence for gluonium content in $\eta'$ (table I, left column). Since the parameters $C_{NS}$, $C_S$, $\varphi_V$ and $m_s/\bar{m}$ were taken from [16], obtained in the hypothesis of no $\eta'$ gluonium content, we repeat the fit adding other $SU(3)$ relations and enlarging the number of free parameters. As shown in table I, the new result is in good agreement for all parameters, confirming the $3\,\sigma$ evidence for gluonium in $\eta'$. The quality of the fit get worse when $Z^2_{\eta'}$ is fixed to zero.

We also investigated the origin of the discrepancy between our result and the one of ref. [17], where a similar fit leads to a null gluonium content in $\eta'$, even if consistent with our measurement. The key point is the use of the $\Gamma(\eta' \to \gamma\gamma)/\Gamma(\pi^0 \to \gamma\gamma)$ constraint in our approach, which significantly increases the central value of $Z^2_{\eta'}$, reducing the error.

TABLE II. – *Fit results for the* $e^+e^- \to \pi^+\pi^-\pi^0\pi^0$ *and* $e^+e^- \to \pi^0\pi^0\gamma$ *cross-sections.*

| Parameter | $4\pi$ channel | $\pi\pi\gamma$ channel |
|---|---|---|
| $\sigma_0$ (nb) | $7.89 \pm 0.06 \pm 0.07$ | $0.724 \pm 0.010 \pm 0.003$ |
| $\Re(Z)$ | $0.106 \pm 0.007 \pm 0.004$ | $0.011 \pm 0.015 \pm 0.006$ |
| $\Im(Z)$ | $-0.103 \pm 0.004 \pm 0.003$ | $-0.154 \pm 0.007 \pm 0.004$ |
| $\sigma'$ (nb/MeV) | $0.064 \pm 0.003 \pm 0.001$ | $0.0053 \pm 0.0005 \pm 0.0002$ |
| $\chi^2/N_{df}$, $P(\chi^2)$ | 4.78/13 (98%) | 11.79/13 (54%) |

## 5. – The $e^+e^- \to \omega\pi^0$ process

In the energy region of few tens of MeV around $M_\phi$, the $\omega\pi^0$ production cross-section is largely dominated by the non-resonant processes $e^+e^- \to \rho/\rho'$. However, in a region closer to $M_\phi$, a contribution from the OZI and $G$-parity–violating decay $\phi \to \omega\pi^0$ is expected. This strongly suppressed decay can be observed only through the interference pattern with the previous reaction, which shows up as a dip in the production cross-section as a function of the center-of-mass energy ($\sqrt{s}$). The interference scheme depends on the final state used in the analysis. For the $\pi^+\pi^-\pi^0\pi^0$ channel only the already mentioned processes are present while for $\pi^0\pi^0\gamma$ there are also contributions from $\phi \to f_0(980)\gamma$ and $\phi \to \rho\pi^0$ which modify the $\sqrt{s}$ behaviour.

The dependence of the cross-section on the center-of-mass energy can be parametrized in the form [19]

$$\sigma(\sqrt{s}) = \sigma_{NR}(\sqrt{s}) \cdot \left| 1 - Z \frac{M_\phi \Gamma_\phi}{D_\phi} \right|^2, \tag{8}$$

where $\sigma_{NR}(\sqrt{s})$ is the bare cross-section for the non-resonant process, $Z$ is a complex interference parameter while $M_\phi$, $\Gamma_\phi$ and $D_\phi$ are the mass, the width and the inverse propagator of the $\phi$-meson, respectively. Since in the considered center-of-mass energy range the non-resonant cross-section increases almost linearly, we assume a simple linear dependence: $\sigma_{NR}(\sqrt{s}) = \sigma_0 + \sigma'(\sqrt{s} - M_\phi)$.

The analysis has been performed on $\sim 600\,\mathrm{pb}^{-1}$ at center-of-mass energies between 1000 and 1030 MeV [20]. For both final states used in this analysis ($\pi^+\pi^-\pi^0\pi^0$ and $\pi^0\pi^0\gamma$) data are filtered by selecting events with the expected signature. After performing a kinematic fit, which improves the energy resolution of photons, specific cuts for background rejection are applied. The measured values of visible cross-section are then fitted using as free parameters $\sigma_0^i$, $\Re(Z_i)$, $\Im(Z_i)$ and $\sigma_i'$, where $i$ is the $4\pi$ or $\pi\pi\gamma$ final state. The values for the extracted parameters are reported in table II. From them we obtain: $\Gamma(\omega \to \pi^0\gamma)/\Gamma(\omega \to \pi^+\pi^-\pi^0) = 0.0897 \pm 0.0016$. Since these two final states correspond to $\sim 98\%$ of the $\omega$ decay channels, this ratio and the sum of the existing $BR$ measurements on the remaining rarer decays [21] are used to extract the main $\omega$ branching fractions imposing the unitarity:

$$BR(\omega \to \pi^+\pi^-\pi^0) = (90.24 \pm 0.19)\%, \tag{9}$$

$$BR(\omega \to \pi^0\gamma) = (8.09 \pm 0.14)\%, \tag{10}$$

with a correlation of $-71\%$.

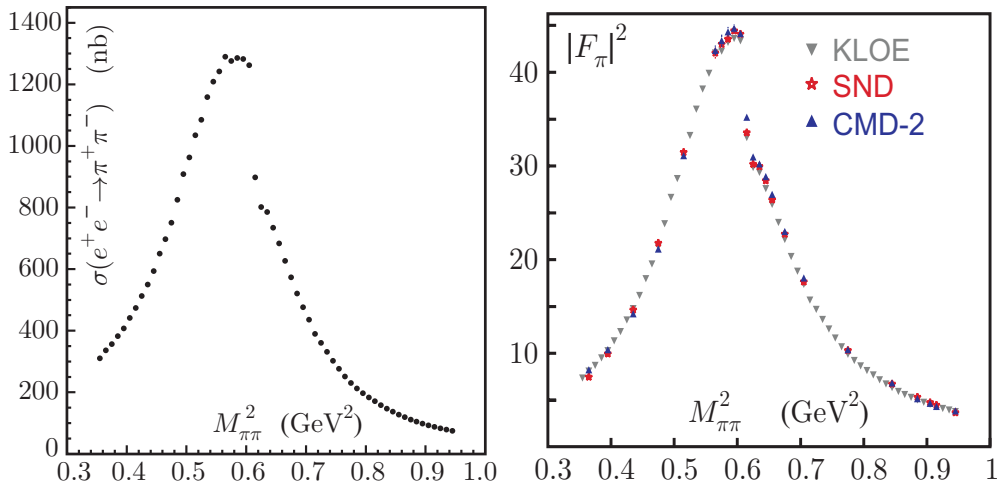


Fig. 3. – Differential cross-section for the process $e^+e^- \to \pi^+\pi^-$ (left) and comparison of the resulting pion form factor with SND and CMD-2 experiments (right).

Using the parameters obtained from the $\pi^+\pi^-\pi^0\pi^0$ analysis, the $\Gamma_{ee}$ measurement from KLOE [22] for the evaluation of $\sigma_\phi$, and our value for $BR(\omega \to \pi^+\pi^-\pi^0)$, we extract

$$BR(\phi \to \omega\pi^0) = (4.4 \pm 0.6) \times 10^{-5}, \tag{11}$$

in agreement and with better accuracy with respect to what obtained by the SND experiment $(5.2^{+1.3}_{-1.1} \times 10^{-5})$ [19].

## 6. – Measurement of $\sigma(e^+e^- \to \pi^+\pi^-\gamma(\gamma))$

The anomalous magnetic moment of the muon has been measured with an accuracy of 0.54 ppm [23]. The main source of uncertainty in the value predicted by the Standard Model is given by the hadronic contribution to the lowest order, $a_\mu^{hlo}$. This quantity can be evaluated via a dispersion integral of the hadronic cross-section measurements. The pion form factor $F_\pi$, proportional to the $\sigma_{\pi\pi}$ cross-section, accounts for $\sim 70\%$ of the central value and for $\sim 60\%$ of the uncertainty in $a_\mu^{hlo}$.

The analysis has been performed on 240 pb$^{-1}$ of data taken at the $\phi$ peak, corresponding to 3.1 Million events [24]. The differential spectrum of the $\pi^+\pi^-$ invariant mass, $M_{\pi\pi}$, is measured from ISR events, $e^+e^- \to \pi^+\pi^-\gamma$, and the total cross-section $\sigma_{\pi\pi}$ is obtained using the formula [25]: $s\,\frac{\mathrm{d}\sigma_{\pi\pi\gamma}}{\mathrm{d}M^2_{\pi\pi}} = \sigma_{\pi\pi}(M^2_{\pi\pi})\; H(M^2_{\pi\pi})$ , where $H$ is the radiator function, describing the photon emission at the initial state. This formula neglects Final State Radiation (FSR) terms, which are however properly taken into account in the analysis.

The analysis requires two charged pion tracks having $50° < \theta_\pi < 130°$ and a photon emitted within a cone of $\theta_\gamma < 15°$ around the beam line. The photon is not explicitly detected and its direction is reconstructed by closing the kinematics of the event. The separation of pion and photon selection regions greatly reduces the contamination from the resonant process $e^+e^- \to \phi \to \pi^+\pi^-\pi^0$, in which the $\pi^0$ mimics the missing momentum of the photon(s) and from FSR. On the other hand, a highly energetic photon emitted at small angle forces the pions also to be at small angles

(and thus outside the selection cuts), resulting in a kinematical suppression of events with $M^2_{\pi\pi} < 0.35\,\mathrm{GeV}^2$. Residual contamination from the processes $\phi \to \pi^+\pi^-\pi^0$ and $e^+e^- \to \mu^+\mu^-\gamma$ is greatly reduced by kinematical cuts, while a particle ID estimator, based on calorimeter information and time-of-flight, is used to suppress the high rate of radiative Bhabhas.

The $\pi\pi\gamma$ differential cross-section (fig. 3 left) is obtained from the observed spectrum after subtracting the residual background events and correcting for the selection efficiency and the luminosity. The total cross-section is then extracted, taking into account next-to-leading–order ISR effects and vacuum polarisation. The cross-section inclusive of FSR is then used to determine $a_\mu^{\pi\pi}$:

$$a_\mu^{\pi\pi}(0.592 < M_{\pi\pi} < 0.975\,\mathrm{GeV}) = (387.2 \pm 3.3) \times 10^{-10}. \tag{12}$$

The total error has a negligible statistical contribution and comparable experimental systematic and theoretical calculation uncertainties (0.6% each). This result is in agreement with CMD-2 and SND values [26, 27], as shown in fig. 3 right, and confirms the current disagreement between the Standard Model prediction for $a_\mu$ and its direct measured value.

REFERENCES


[1] Ambrosino F. *et al.* (KLOE Collaboration), *Phys. Lett. B*, **681** (2009) 5.
[2] Achasov N. N. and Gubin V. V., *Phys. Rev. D*, **56** (1997) 4084.
[3] Isidori G., Maiani L., Nicolaci M. and Pacetti S., *JHEP*, **0605** (2006) 049.
[4] Ambrosino F. *et al.* (KLOE Collaboration), *Phys. Lett. B*, **679** (2009) 10.
[5] Ambrosino F. *et al.* (KLOE Collaboration), *Phys. Lett. B*, **634** (2006) 148.
[6] Ambrosino F. *et al.* (KLOE Collaboration), *Eur. Phys. J. C*, **49** (2007) 473.
[7] Landsberg L. G., *Phys. Rep.*, **128** (1985) 301.
[8] Jarlskog C. and Pilkuhn H., *Nucl. Phys. B*, **1** (1967) 264.
[9] Faessler A., Fuchs C. and Krivoruchenko M. I., *Phys. Rev. C*, **61** (2000) 035206.
[10] Picciotto C. and Richardson S., *Phys. Rev. D*, **48** (1993) 3395.
[11] Borasoy B. and Nissler R., *Eur. Phys. J. A*, **33** (2007) 95.
[12] Gao D. N., *Mod. Phys. Lett. A*, **17** (2002) 1583.
[13] Ambrosino F. *et al.* (KLOE Collaboration), *Phys. Lett. B*, **675** (2009) 283.
[14] Rosner J. L., *Phys. Rev. D*, **27** (1983) 1101.
[15] Ambrosino F. *et al.* (KLOE Collaboration), *Phys. Lett. B*, **648** (2007) 267.
[16] Bramon A., Escribano R. and Scadron M. D., *Phys. Lett. B*, **503** (2001) 271.
[17] Escribano R. and Nadal J., *JHEP*, **05** (2007) 6.
[18] Kuo E., *Phys. Rev. D*, **63** (2001) 054027.
[19] Aulchenko V. M. *et al.*, *J. Exp. Theor. Phys.*, **90** (2000) 927.
[20] Ambrosino F. *et al.* (KLOE Collaboration), *Phys. Lett. B*, **669** (2008) 223.
[21] Yao W. M. *et al.*, *J. Phys. G*, **33** (2006) 1 and 2007 partial update for 2008 edition [`http://pdg.web.cern.ch/pdg`].
[22] Ambrosino F. *et al.* (KLOE Collaboration), *Phys. Lett. B*, **608** (2005) 199.
[23] Bennett G. W. *et al.* (Muon g-2 Collaboration), *Phys. Rev. D*, **73** (2006) 072003.
[24] Ambrosino A. *et al.* (KLOE Collaboration), *Phys. Lett. B*, **670** (2009) 285.
[25] Binner S., Kühn J. H. and Melnikov K., *Phys. Lett. B*, **459** (1999) 279.
[26] Achasov M. N. *et al.* (SND Collaboration), *J. Exp. Theor. Phys.*, **103** (2006) 380.
[27] Akhmetshin R. R. *et al.* (CMD-2 Collaboration), *Phys. Lett. B*, **648** (2007) 28.